Published in final edited form as:
Neurobiol Dis. 2012 August ; 47(2): 155–162. doi:10.1016/j.nbd.2012.03.033.

Neurogenic abnormalities in Alzheimer's disease differ between stages of neurogenesis and are partly related to cholinergic pathology

Elaine K. Perry[a], **Mary Johnson**[a], **Antigoni Ekonomou**[b], **Robert H. Perry**[a], **Clive Ballard**[b], and **Johannes Attems**[a,*]

[a]Institute for Ageing and Health, Newcastle University, Campus for Ageing and Vitality, Newcastle upon Tyne, NE4 5PL, UK

[b]Wolfson Centre for Age Related Diseases, King's College London, Guys Campus, London, SE1 1UL, UK

Abstract

Neurogenesis occurs in the subventricular zone and the sub-granular layer of the hippocampus and is thought to take place in 5 stages, including proliferation, differentiation, migration, targeting, and integration phases, respectively. In Alzheimer's disease (AD) both increased and decreased neurogenesis has been reported and cholinergic activity is assumed to be involved in neurogenesis. The aim of this study was to systematically assess different phases of neurogenesis and their relation to AD and cholinergic pathology. We investigated *post-mortem* brain tissue from 20 AD patients and 21 non-demented controls that was neuropathologically characterized according to standardized criteria. Hippocampal sections were stained with antibodies against neurogenic markers Musashi-1, nestin, PSA-NCAM, doublecortin, and β-III-tubulin as well as ChAT (choline-acetyltransferase). Using image analysis immunoreactivity was assessed in the subventricular zone, the sub-granular layer, and the granule cell layer by determining the integrated optical density.

In the sub-granular layer and the granule cell layer Musashi-1 and ChAT immunoreactivities were significantly lower in AD and decreased with increasing Braak stages. Conversely, immunorreactivities of both nestin and PSA-NCAM were significantly higher in AD and increased with increasing Braak stages while no changes were seen for doublecortin and β-III-tubulin, except for significantly higher doublecortin levels in the granule cell layer of AD cases. Of note, Musashi-1 immunoreactivity significantly correlated with ChAT immuonoreactivity across different Braak stages. In the subventricular zone only nestin immunoreactivity was significantly higher in AD and significantly increased with increasing Braak stages, while no significant differences were seen for all other markers.

Our finding of a reduction of ChAT and Musashi-1 levels in AD is compatible with the assumption that cholinergic pathology *per se* has a detrimental influence on neurogenesis. We conclude that neurogenic abnormalities in AD differ between phases and areas of neurogenesis

*Corresponding author. Fax: +44 191 248 1301. j.attems@ncl.ac.uk (J. Attems).

Europe PMC Funders Author Manuscripts

and stages of AD; while hippocampal stem cells (Musashi-1) decrease, proliferation (nestin) increases and differentiation/migration phase as well as axonal/dendritic targeting (doublecortin and β-III-tubulin) remains virtually unchanged. This suggests an attenuation of stem cells together with compensatory increased proliferation that, however, does not result in an increased number of migratory neuroblasts and differentiated neurons in AD.

Keywords

Alzheimer's disease; Neurogenesis; Musashi-1; Cholinergic pathology; Nestin

Introduction

Neurogenesis (NG) occurs throughout life in the brain of adult mammals in the subventricular zone (SVZ) of the lateral ventricles including a layer in the ventral temporal horn overlying the hippocampus (Bird et al., 1983; Curtis et al., 2007; Drapeau et al., 2003) and in the sub-granular layer (SGL) of the dentate gyrus (Eriksson et al., 1998). Neuroblasts from the SVZ constitute the rostral migratory stream (RMS) which terminates in the olfactory bulb where those neuroblasts mature into GABA-ergic interneurons (Bedard and Parent, 2004; Birks et al., 2009) while neurons born in the adult SGL migrate into the granule cell layer (GL) of the dentate gyrus and mature into dentate granule cells (Crespel et al., 2005).

The process of NG is thought to take place in 5 stages (von Bohlen Und Halbach, 2007) and in hippocampal NG proliferative precursor cell stages, characterized by the presence of type-1, type-2, and type-3 cells, as well as postmitotic stages can be distinguished (Kempermann et al., 2004; Kempermann, 2011). Briefly, stage 1 (proliferation phase) is characterized by stem cells or progenitor cells that are positive for glial fibrillary acidic protein (GFAP) and nestin (Fukuda et al., 2003), the latter being a key marker of undifferentiated neuronal progenitor cells (Bernier et al., 2000). In addition Musashi-1 (Msi-1), an RNA binding protein involved in the Notch pathway via repression of Notch inhibiting m-Numb (Imai et al., 2001; Sakakibara et al., 1996), is expressed in neural progenitor cells including stem cells (Maslov et al., 2004; Sakakibara et al., 1996). The immunoreactive pattern of stage 1 corresponds to type-1 cells of hippocampal NG. However, type-1 cells represent stem cells and only 5% of cell divisions among nestin-expressing cells of the SGL are in type-1 cells (Kronenberg et al., 2003). Hence, type-1 cells do not have a highly proliferative capacity. In early stage 2 (differentiation phase) cells express nestin while at later time-points of stage 2 cells cease expressing nestin and start expressing doublecortin and polysialynated embryonic neural cell adhesion molecule (PSA-NCAM) (Fukuda et al., 2003; Kronenberg et al., 2003); PSA-NCAM is a cell surface glycoprotein involved in neural migration, neurite growth, and axonal branching during development and adulthood (Seki and Arai, 1993). In the hippocampus, stage 2 is thereby characterized by type-2 cells that are termed transiently amplifying progenitor cells (Kempermann, 2011) and are subdivided into type-2a and type-2b cells; both subtypes express nestin while only type-2b cells express doublecortin and PSA-NCAM. Type-2 cells are highly proliferative with type-2b cells being neuronally determined (Kempermann et al.,

Europe PMC Funders Author Manuscripts

2004). In stage 3 (migration phase) type-3 cells, that are neuroblasts exhibiting first dendrites, express doublecortin, PSA-NCAM (Kempermann, 2011), and β-III-tubulin (Seri et al., 2004). These markers are also expressed in stage 4 (axonal and dendritic targeting) together with calretinin and neuron-specific nuclear protein (NeuN) (Brandt et al., 2003; Kempermann et al., 2004; Llorens-Martin et al., 2006; Ming and Song, 2005). In stage 5 (synaptic integration) neurons are positive for NeuN and Calbindin (Brandt et al., 2003; Kempermann et al., 2004). Stages 4 and 5 are postmitotic stages (Kempermann et al., 2004).

NG represents a key factor in plasticity of adult brain in response to environmental stimuli (Ge et al., 2006) and abnormalities in NG have been detected in neurodegenerative diseases such as Alzheimer's disease (AD) (Winner et al., 2011). Using doublecortin and PSA-NCAM staining Jin et al. (2004) demonstrated a significant increase in SGL neurogenesis in *post-mortem* brains of AD patients. On the other hand, a decline in the extent of proliferation of progenitor cells and their numbers has been suggested in AD (Brinton and Wang, 2006) and reductions in the proliferative marker Msi-1 in the SGL has been observed in both AD (Ziabreva et al., 2006) and dementia with Lewy bodies (Johnson et al., 2011). It was suggested recently that synaptic pathology and defective NG are related to progressive accumulation of amyloid-β protein (Aβ) oligomers in AD; Aβ may activate cyclin-dependent kinase 5 (CDK5), which plays a role in synaptic function and neuronal integrity, thereby impairing neuronal maturation in NG (Crews and Masliah, 2010). Similarly, NG might be impaired by the intracellular domain (AICD) of the amyloid precursor protein (APP) that is generated by the γ-secretase processing of APP (Ghosal et al., 2010).

Both the increase and decrease in NG have been described in transgenic mice that partly recapitulate AD pathology; long lasting impairment of NG is associated with amyloid deposition in a transgenic knock in a mouse model of familial AD (Zhang et al., 2007) while increased hippocampal NG was seen in the in APP/PS1 double transgenic mice (Yu et al., 2009). Reductions in NG and high levels of hyperphosphorylated tau in NG areas have been demonstrated in transgenic mice harboring familial AD-linked mutant APPswe/PS1DeltaE9 (Demars et al., 2010). Using the triple transgenic (3xTG) AD mouse model that generates both Aβ and tau pathology Hamilton et al. (2010) found in NG areas decreased numbers of proliferating cells, early lineage neural progenitors and neuroblasts at middle (11 months old) and old age (18 months old). These findings indicate that AD-associated mutations suppress NG early during disease development (Hamilton et al., 2010).

Cholinergic activity is assumed to be involved in NG as it is likely to be functionally important in controlling the generation of neural stem cells in adult brains since cholinergic drugs influence proliferative activity in these regions (Cooper-Kuhn et al., 2004). In both AD and dementias related to α-synuclein pathology there is evidence of a relationship between reduced progenitor activity and cortical cholinergic loss (Cooper-Kuhn et al., 2004), consistent with experimental animal studies demonstrating that lesions in ascending cholinergic tracts significantly reduce NG (Contestabile and Ciani, 2008).

However, data on the relation between cholinergic pathology and NG in hippocampal NG areas in AD are lacking; we therefore aimed to systematically investigate different stages of

NG and cholineacetyltransferase (ChAT) immunoreactivity in hippocampal NG areas of *post-mortem* brains from both non-demented individuals and AD patients.

Material and methods

Brain tissue from 20 AD patients (mean age, 81.2±7.0 years; 13 female) and 21 age matched non-demented controls (mean age, 80.9±8.5 years; 13 female) was obtained from the Newcastle Brain Tissue Resource (NBTR). Brains were donated between 1982 and 2004 and collected in accordance with the approval of the Joint Ethics Committee of Newcastle and North Tyneside Health Authority and following NBTR brain banking procedures. There was no significant difference in age, gender or post-mortem delays between the groups (Table 1). AD cases had a clinical diagnosis of AD according to NINCDS-ADRA (McKhann et al., 1984) criteria and fulfilled the neuropathological criteria for Braak stage IV, V or VI (Braak and Braak, 1991; Braak et al., 2006) and CERAD “moderate” or “severe” (Mirra et al., 1993) resulting in a diagnosis of medium or high likelihood of AD according to NIA-Reagan Institute Criteria (Hyman, 1998). Control cases did not show any clinical signs of psychiatric or neurological disease and had Braak stage I, II or III and CERAD “negative” or “mild”. According to recently published National Institute on Aging —Alzheimer’s Association (NIA-AA) guidelines (Montine et al., 2011) the level of AD neuropathologic change in the 21 non-demented control cases included “Not” (n=5), “Low” (n=14) and “Intermediate” (n=2) while it ranged from “Intermediate” (n=6) to “High” (n=14) in the 20 AD cases.

Neuropathological examination was performed according to a standard protocol: Brains were fixed in 4% formaldehyde solution for 4 weeks. Paraffin embedded blocks from mid-frontal, frontobasal, superior temporal, inferior parietal, and occipital cortex, hippocampus with entorhinal cortex, cingulate gyrus, basal ganglia, amygdala, mesencephalon, pons, medulla oblongata (at two transverse levels), and cerebellum were examined using routine stains (H&E, cresyl violet, Kluver–Barrera), modified Bielschowsky’s silver stain, and immunohistochemistry for amyloid-β (Aβ) peptide (clone 4G8, Signet Labs, Dedham, MA, USA), phosphorylated tau protein (antibody AT-8; Innogenetics, Ghent, Belgium), and α-synuclein (Chemicon, Hofheim, Germany). Neuropathological diagnoses were made according to established postmortem consensus criteria, for AD including Braak staging (Braak and Braak, 1991; Braak et al., 2006), CERAD scores (Mirra et al., 1993) and Thal Aβ phases (Thal et al., 2002).

Immunohistochemistry for NG markers and ChAT was performed blind to group categories. From paraffin embedded tissue blocks containing the posterior hippocampus at the level of the lateral geniculate nucleus that were used for routine neuropathological assessment (e.g., tau pathology for Braak stages) 6 consecutive 10 μm microtome sections were stained with antibodies against Msi-1 (rabbit polyclonal, Chemicon), nestin (rabbit polyclonal, Chemicon), PSA-NCAM (mouse monoclonal, Dako, Glostru p, Denmark), ChAT (goat polyclonal, Chemicon), doublecortin (rabbit poyclonal, Abcam) and β-III-tubulin (mouse monoclonal, Sigma), respectively. Antigen unmasking was performed using pressure cooking in 0.1 mol/L EDTA for 1 min (ChAT, doublecortin, β-III-tubulin) or microwaving in 0.01 mol/L citrate buffer for 10 min (Msi-1, nestin, PSA-NCAM), prior to incubation

with the primary antibody. The immunoreactive product was visualized by nickel enhanced 3,3-diaminobenzidine (ChAT) and DAB/peroxide (Msi-1, nestin, PSA-NCAM, doublecortin, β-III-tubulin). In a subset of cases (n=9) hematoxylin counterstain was performed on ChAT section to better visualize neuronal nuclei. Control sections were assessed without the primary antibody and all were free of immunostaining.

Immunoreactivity of each ChAT, Msi-1, nestin, PSA-NCAM, double-cortin, and β-III-tubulin was assessed in the hippocampal NG areas i.e., SVZ and SGL as well as GL to which SGL neural stem cells migrate. Five randomly selected digital images from each SVZ, SGL and GL were scanned for immunoreactivity.

Images were captured using a JVC 3-chip CCD true color camera mounted on Zeiss Axioplan 2 bright field photo-microscope and Neotech Image Grabber software. IHC was quantified using Image Pro Plus v.4.1 image analysis system: RGB thresholding was set to include immunopositivity of both neuronal somata and neuronal cell processes in the neuropil but to exclude unspecific background staining. RGB thresholding was standardized for each antibody separately and the integrated optical density (IOD) was assessed.

As our data were not normally distributed (Kolmogorov–Smirnov, $P<0.01$) we used non-parametric tests for statistical evaluation: IODs of each ChAT, Msi-1, nestin, PSA-NCAM, doublecortin, and β-III-tubulin immunoreactivity in all investigated regions were compared between AD and controls (Mann–Whitney U) and between Braak stages I–VI (non-parametric *t*-test). Correlations between Braak stages and IODs were analyzed by calculating Spearman's rank correlation coefficient. For all statistical evaluations we used SPSS version 17.

Results

Msi-1 stained small, undifferentiated cells in SVZ, SGL, and GL, including neuronal processes (Figs. 1A, F, K, and P). In the total study group Msi-1 IOD was highest in SVZ followed by GL and SGL (Table 2). In both SGL and GL but not in SVZ Msi-1 IOD was significantly lower in AD compared to controls (Table 2) and negatively correlated with Braak stages (SGL, $rho=-0.413$, $P<0.01$; GL, $rho=-0.556$, $P<0.01$, Figs. 2A–C). In SGL and GL Msi-1 IOD was significantly lower in Braak stage VI compared to Braak stages I–III ($P<0.05$, Figs. 2B–C) and in GL additional significant differences were seen between Braak stage IV and I–II ($P<0.05$, Fig. 2C). No respective differences were seen in SVZ and in all areas Msi-1 IOD increased from Braak stage I to II ($P>0.05$, Figs. 2 A–C).

Nestin IOD was highest in SVZ followed by SGL and GL and in all investigated areas significantly higher in AD compared to controls (Table 2; Figs. 1B, G, L, and Q). Overall we have seen a significant increase in nestin IOD with increasing Braak stages (SVZ, $rho=0.666$, $P<0.01$; SGL, $rho=0.377$, $P<0.05$; GL, $rho=0.646$, $P<0.01$) but in SGL and GL nestin IOD was lower in Braak stage II compared to Braak stage I ($P>0.05$, Figs. 2D–F). In SVZ nestin IOD was significantly higher in Braak stages V and VI compared to I–IV ($P<0.05$, Fig. 2D), in SGL in V and VI compared to I–III, respectively ($P<0.05$, Fig. 2C)

while differences in GL were significant between V and VI compared to II and between V and III (P<0.05, Fig. 2E).

PSA-NCAM immunostaining revealed punctate precipitates in neuronal cell bodies and neuropil (Figs. 1C, H, M, and R) and PSA-NCAM IOD was highest in SGL followed by GL and SVZ (Table 2). In SGL and GL but not in SVZ PSA-NCAM IOD was significantly higher in AD compared to controls (P<0.01, Table 2) and correlated with Braak stages (SGL, rho=0.489, P<0.01; GL, rho=0.526, P<0.01; Figs. 2G–I). In both SGL and GL PSA-NCAM IODs were significantly higher in Braak stage VI compared to I–III (P<0.05; Figs. 2H–I), no other respective differences were seen.

Doublecortin immunostaining was present to a similar degree in all regions (Table 2) and showed a predominately cytoplasmic staining pattern (Figs. 1D, I, N, and S). Doublecortin IOD was significantly higher (P<0.01) in AD compared to controls in the GL only, where significant respective differences have been seen between Braak stages IV and II/III and between Braak stages V and III (P<0.05; Figs. 2J–L).

β-III-tubulin immunoreactivity was present in both cell bodies and processes (Figs. 1E, J, O, and T) and its IOD was highest in SVZ followed by GL and SGL (Table 2). No significant differences were seen between AD and controls (Table 2) and between different Braak stages (Figs. 2M–O).

ChAT immunostaining was generally present in neurons and in the neuropil of all investigated areas. Cellular immunopositivity presented as strong globular cytoplasmic staining filling the entire cytoplasm (Fig. 3D) or as granular cytoplasmic staining as well as faint diffuse cytoplasmic staining while in the neuropil thread- and small dot-like immunopositive axons and dendrites were seen (Fig. 3). ChAT IOD was highest in SGL followed by SVZ and GL (Table 2). ChAT IOD in AD was significantly lower compared to controls (P<0.001) and significantly decreased with increasing Braak stages in SGL and GL (SGL, rho= −0.898; GL, rho=−0.79; P<0.001) while no significant differences were seen in SVZ (Fig. 4). In SGL ChAT IOD was significantly lower in Braak stages IV–VI and in GL in V–VI compared to I–III, respectively (P<0.05, Figs. 4B–C), while an additional significant difference was seen in GL between Braak stages IV and I (P<0.05, Fig. 4C).

IODs of PSA-NCAM and nestin negatively correlated in the SVZ (rho=−0.36, P<0.05) while a positive correlation was seen in GL (rho=0.444, P<0.05); no other correlations between PSA-NCAM, nestin, Msi-1, doublecortin, and β-III-tubulin were observed in any of the NG niche areas. Of note, Msi-1 was the only NG marker that correlated with ChAT as Msi-1 IOD significantly decreased with decreasing ChAT IOD in SGL and GL (SGL, rho=0.593, P<0.01; GL, rho=0.735, P<0.01).

Fig. 5 shows the neuropathological hallmark lesions for AD in NG areas; while Aβ plaques (Fig. 5B) as well as neuritic plaques (Fig. 5D) and neurofibrillary tangles (Figs. 5A, C–D) are absent in all NG niche areas, hyperphosphorylated microtubule-associated protein tau in the form of neuropil threads and pretangles is seen in both SGL and GL (Figs. 5A, C).

Discussion

The results of our study indicate that changes in hippocampal NG in AD differ between NG phases, NG niche areas and AD stages; while progenitor/stem cell marker Msi-1 (type-1 cells; proliferation phase) decreases, nestin (type-2a and -2b cells; differentiation phase) and to a lesser degree PSA-NCAM (type-2b and -3 cells; differentiation/migration phase and axonal/dendritic targeting) increase with the progression of AD (increasing Braak stages). On the other hand, no significant differences were seen in the expression of β-III-tubulin (type-3 cells; migration phase and axonal/dendritic targeting) between different stages of AD and doublecortin was higher in AD compared to controls in the GL only, but showed no correlation with Braak stages. With respect to other regional variations, in both SGL and GL significant differences between AD and controls regarding Msi-1, nestin and PSA-NCAM IODs were seen while in the SVZ only nestin IOD was significantly higher in AD. NG in the SGL, although less active than in the SVZ (Curtis etal., 2011), is of particular interest in AD since new-born neurons integrating into the dentate gyrus as a function of activity or experience are vital for memory function (Aasebo et al., 2011; Koehl and Abrous, 2011; Mongiat and Schinder, 2011).

Increased nestin immunoreactivity in higher Braak stages could potentially indicate an increase in type-1, type-2a, and type 2b cells that characterize the first two stages of NG (i.e., proliferation and differentiation phases) (Kempermann et al., 2004). However, we have seen a decrease in Msi-1 immunoreactivity in higher Braak stages indicating a reduction in the number of hippocampal stem cells (type-1 cells) in AD while PSA-NCAM and doublecortin that are additional markers for type-2b cells (Kempermann, 2011) showed an ambiguous pattern of immunoreactivity; in both SGL and GL PSA-NCAM increased with increasing Braak stages and was significantly higher in AD compared to controls. Doublecortin on the other hand, did not significantly increase with increasing Braak stages but in the GL was significantly higher in AD compared to controls. Thereby, the finding of an increase in nestin immunoreactivity suggests that predominately type-2a cells that characterize proliferating cells without neuronal determination and to a lesser extend neuronally determined type-2b cells increase with increasing AD pathology. The lack of a change in β-III-tubulin expression with increasing Braak stages suggests despite respective increases in both PSA-NCAM and doublecortin, that NG stages 3 (migration phase; type 3 cells) and 4 (axonal and dendritic targeting; postmitotic stage) remain unchanged in AD. Hence, we suggest that in AD hippocampal stem cells decrease while transiently amplifying progenitor cells including neuronally determined cells increase. However, while the increase in type-2 cells might reflect a compensatory mechanism it does not result in increased migration or axonal and dendritic targeting as type-3 cells and postmitotic stages remain stable.

In relation to disease staging increased nestin and PSA-NCAM and decreased Msi-1 appear to be later disease stage phenomena. However Msi-1 IOD was increased in Braak stage 2 indicating a transient increase at earlier, preclinical stages of AD that could reflect initial compensatory mechanisms. Such compensatory mechanisms may be initiated by alteration of the environment in the NG areas that initially may stimulate NG but become inhibitory once an environmental threshold is passed and neuropathological changes (e.g.,

hyperphosphorylation of tau) develop. This has been indicated by Shruster et al. (2010) in relation to amyloidosis. Our results clearly indicate that changes in the expression of NG markers relate to the stage of AD pathology as reflected by the severity of tau pathology (Braak stages); this might point towards an association between NG and tau pathology.

While increased nestin immunoreactivity in higher Braak stages indicates a compensatory increase of proliferation, it is unclear if the reduction in stem cell number as reflected by reduced Msi-1 immunoreactivity with increasing tau pathology is a result of tau toxicity or conversely may cause/aggravate tau pathology. The latter has been suggested for AD in both humans and animal models (Demars et al., 2010; Lazarov and Marr, 2010; Winner et al., 2011).

In this study it is demonstrated for the first time that in SGL and GL ChAT IOD decreases with increasing tau pathology suggesting an association between AD pathology and cholinergic pathology in human hippocampal NG areas. The reduction of ChAT IOD significantly correlated with the reduction of Msi-1 IOD suggesting an association between progenitor activity and cholinergic activity. Acetylcholine has indeed been shown to play a role in NG; animal model studies indicate that the cholinergic system plays a key survival-promoting role for neuronal progenitors and immature neurons within regions of adult NG. Following immunotoxin 192IgG-saporin injection in lateral ventricles of adult rats to selectively lesion cholinergic neurons of the cholinergic basal forebrain, NG declined significantly in GL and olfactory bulb (Cooper-Kuhn et al., 2004). Selective neurotoxic lesion of forebrain cholinergic input with 192 IgG-saporin reduces NG in the dentate gyrus with concurrent impairment in spatial memory (Mohapel et al., 2005). Conversely, systemic administration of the cholinergic agonist physostigmine increases NG. Forebrain acetylcholine levels primarily influence proliferation and/or the short-term survival rather than long-term survival or differentiation of new neurons (Mohapel et al., 2005). Therefore, the reduction of ChAT and Msi-1 levels in AD might suggest that cholinergic pathology *per se* has a detrimental influence on NG.

We conclude that NG abnormalities in AD do not follow a uniform pattern but vary considerably between stages and NG niche areas as well as disease stage. This conclusion is relevant for the interpretation of previous respective studies that reported both increased and decreased NG in AD and for the design of future studies aiming to further elucidate the association between NG and AD. Our finding of a significant association between reduced hippocampal stem cells and reduced ChAT levels warrants further studies on the impact of cholinergic pathology on NG in AD.

Acknowledgments

The authors are grateful to Dr. Alan Alpar and Prof. Tibor Harkany, Karolinska Institutet, for reading this manuscript and providing us with helpful comments. This study was supported by a pilot and an equipment grant from the Alzheimer Research Trust and the Newcastle NIHR Biomedical Research Centre In Ageing and Age Related Diseases. Tissue for this study was provided by the Newcastle Brain Tissue Resource, which is funded in part by a grant from the UK Medical Research Council (G0400074). This work was also supported by the UK NIHR Biomedical Research Centre for Ageing and Age-related disease award to the Newcastle upon Tyne Hospitals NHS Foundation Trust and by a grant from the Alzheimer's Society and Alzheimer's Research Trust as part of the brains for Dementia Research Project.

Europe PMC Funders Author Manuscripts

References

Aasebo IE, Blankvoort S, Tashiro A. Critical maturational period of new neurons in adult dentate gyrus for their involvement in memory formation. Eur. J. Neurosci. 2011; 33:1094–1100. [PubMed: 21395853]

Bedard A, Parent A. Evidence of newly generated neurons in the human olfactory bulb. Brain Res. Dev. Brain Res. 2004; 151:159–168.

Bernier PJ, Vinet J, Cossette M, Parent A. Characterization of the subventricular zone of the adult human brain: evidence for the involvement of Bcl-2. Neurosci. Res. 2000; 37:67–78. [PubMed: 10802345]

Bird TD, Stranahan S, Sumi SM, Raskind M. Alzheimer's disease: choline acetyltransferase activity in brain tissue from clinical and pathological subgroups. Ann. Neurol. 1983; 14:284–293. [PubMed: 6227276]

Birks J, Grimley Evans J, Iakovidou V, Tsolaki M, Holt FE. Rivastigmine for Alzheimer's disease. Cochrane Database Syst. Rev. 2009:CD001191. [PubMed: 19370562]

Braak H, Braak E. Neuropathological stageing of Alzheimer-related changes. Acta Neuropathol. 1991; 82:239–259. [PubMed: 1759558]

Braak H, Alafuzoff I, Arzberger T, Kretzschmar H, Del Tredici K. Staging of Alzheimer disease-associated neurofibrillary pathology using paraffin sections and immunocytochemistry. Acta Neuropathol. 2006; 112:389–404. [PubMed: 16906426]

Brandt MD, Jessberger S, Steiner B, Kronenberg G, Reuter K, Bick-Sander A, von der Behrens W, Kempermann G. Transient calretinin expression defines early postmitotic step of neuronal differentiation in adult hippocampal neurogenesis of mice. Mol. Cell. Neurosci. 2003; 24:603–613. [PubMed: 14664811]

Brinton RD, Wang JM. Therapeutic potential of neurogenesis for prevention and recovery from Alzheimer's disease: allopregnanolone as a proof of concept neurogenic agent. Curr. Alzheimer Res. 2006; 3:185–190. [PubMed: 16842093]

Contestabile A, Ciani E. The place of choline acetyltransferase activity measurement in the "cholinergic hypothesis" of neurodegenerative diseases. Neurochem. Res. 2008; 33:318–327. [PubMed: 17940885]

Cooper-Kuhn CM, Winkler J, Kuhn HG. Decreased neurogenesis after cholinergic forebrain lesion in the adult rat. J. Neurosci. Res. 2004; 77:155–165. [PubMed: 15211583]

Crespel A, Rigau V, Coubes P, Rousset MC, de Bock F, Okano H, et al. Increased number of neural progenitors in human temporal lobe epilepsy. Neurobiol. Dis. 2005; 19:436–450. [PubMed: 16023586]

Crews L, Masliah E. Molecular mechanisms of neurodegeneration in Alzheimer's disease. Hum. Mol. Genet. 2010; 19:R12–R20. [PubMed: 20413653]

Curtis MA, Kam M, Nannmark U, Anderson MF, Axell MZ, Wikkelso C, et al. Human neuroblasts migrate to the olfactory bulb via a lateral ventricular extension. Science. 2007; 315:1243–1249. [PubMed: 17303719]

Curtis MA, Kam M, Faull RL. Neurogenesis in humans. Eur. J. Neurosci. 2011; 33:1170–1174. [PubMed: 21395861]

Demars M, Hu YS, Gadadhar A, Lazarov O. Impaired neurogenesis is an early event in the etiology of familial Alzheimer's disease in transgenic mice. J. Neurosci. Res. 2010; 88:2103–2117. [PubMed: 20209626]

Drapeau E, Mayo W, Aurousseau C, Le Moal M, Piazza PV, Abrous DN. Spatial memory performances of aged rats in the water maze predict levels of hippocampal neurogenesis. Proc. Natl. Acad. Sci. U. S. A. 2003; 100:14385–14390. [PubMed: 14614143]

Eriksson PS, Perfilieva E, Bjork-Eriksson T, Alborn AM, Nordborg C, Peterson DA, et al. Neurogenesis in the adult human hippocampus. Nat. Med. Nov.1998 4(11):1313–1317. [PubMed: 9809557]

Fukuda S, Kato F, Tozuka Y, Yamaguchi M, Miyamoto Y, Hisatsune T. Two distinct subpopulations of nestin-positive cells in adult mouse dentate gyrus. J. Neurosci. 2003; 23:9357–9366. [PubMed: 14561863]

Ge S, Goh EL, Sailor KA, Kitabatake Y, Ming GL, Song H. GABA regulates synaptic integration of newly generated neurons in the adult brain. Nature. 2006; 439:589–593. [PubMed: 16341203]

Ghosal K, Stathopoulos A, Pimplikar SW. APP intracellular domain impairs adult neurogenesis in transgenic mice by inducing neuroinflammation. PLoS One. 2010; 5:e11866. [PubMed: 20689579]

Hamilton LK, Aumont A, Julien C, Vadnais A, Calon F, Fernandes KJ. Widespread deficits in adult neurogenesis precede plaque and tangle formation in the 3xTg mouse model of Alzheimer's disease. Eur. J. Neurosci. 2010; 32:905–920. [PubMed: 20726889]

Hyman BT. New neuropathological criteria for Alzheimer disease. Arch. Neurol. 1998; 55:1174–1176. [PubMed: 9740109]

Imai T, Tokunaga A, Yoshida T, Hashimoto M, Mikoshiba K, Weinmaster G, et al. The neural RNA-binding protein Musashi1 translationally regulates mammalian numb gene expression by interacting with its mRNA. Mol. Cell. Biol. 2001; 21:3888–3900. [PubMed: 11359897]

Jin K, Peel AL, Mao XO, Xie L, Cottrell BA, Henshall DC, et al. Increased hippocampal neurogenesis in Alzheimer's disease. Proc. Natl. Acad. Sci. U. S. A. 2004; 101:343–347. [PubMed: 14660786]

Johnson M, Ekonomou A, Hobbs C, Ballard CG, Perry RH, Perry EK. Neurogenic marker abnormalities in the hippocampus in dementia with Lewy bodies. Hippocampus. 2011; 21:1126–1136. [PubMed: 20665591]

Kempermann, G. Adult hippocampal neurogenesis. In: Kempermann, G., editor. Adult neurogenesis 2. 2nd ed. Oxford University Press; New York: 2011. p. 185-215.

Kempermann G, Jessberger S, Steiner B, Kronenberg G. Milestones of neuronal development in the adult hippocampus. Trends Neurosci. 2004; 27:447–452. [PubMed: 15271491]

Koehl M, Abrous DN. A new chapter in the field of memory: adult hippocampal neurogenesis. Eur. J. Neurosci. 2011; 33:1101–1114. [PubMed: 21395854]

Kronenberg G, Reuter K, Steiner B, Brandt MD, Jessberger S, Yamaguchi M, Kempermann G. Subpopulations of proliferating cells of the adult hippocampus respond differently to physiologic neurogenic stimuli. J. Comp. Neurol. 2003; 467:455–463. [PubMed: 14624480]

Lazarov O, Marr RA. Neurogenesis and Alzheimer's disease: at the crossroads. Exp. Neurol. 2010; 223:267–281. [PubMed: 19699201]

Llorens-Martin M, Torres-Aleman I, Trejo JL. Pronounced individual variation in the response to the stimulatory action of exercise on immature hippocampal neurons. Hippocampus. 2006; 16:480–490. [PubMed: 16596582]

Maslov AY, Barone TA, Plunkett RJ, Pruitt SC. Neural stem cell detection, characterization, and age-related changes in the subventricular zone of mice. J. Neurosci. 2004; 24:1726–1733. [PubMed: 14973255]

McKhann G, Drachman D, Folstein M, Katzman R, Price D, Stadlan EM. Clinical diagnosis of Alzheimer's disease: report of the NINCDS-ADRDA Work Group under the auspices of Department of Health and Human Services Task Force on Alzheimer's Disease. Neurology. 1984; 34:939–944. [PubMed: 6610841]

Ming GL, Song H. Adult neurogenesis in the mammalian central nervous system. Annu. Rev. Neurosci. 2005; 28:223–250. [PubMed: 16022595]

Mirra SS, Hart MN, Terry RD. Making the diagnosis of Alzheimer's disease. A primer for practicing pathologists. Arch. Pathol. Lab. Med. 1993; 117:132–144. [PubMed: 8427562]

Mohapel P, Leanza G, Kokaia M, Lindvall O. Forebrain acetylcholine regulates adult hippocampal neurogenesis and learning. Neurobiol. Aging. 2005; 26:939–946. [PubMed: 15718053]

Mongiat LA, Schinder AF. Adult neurogenesis and the plasticity of the dentate gyrus network. Eur. J. Neurosci. 2011; 33:1055–1061. [PubMed: 21395848]

Montine TJ, Phelps CH, Beach TG, Bigio EH, Cairns NJ, Dickson DW, et al. National Institute on Aging-Alzheimer's Association guidelines for the neuropathologic assessment of Alzheimer's disease: a practical approach. Acta Neuropathol. 2011; 123:1–11. [PubMed: 22101365]

Sakakibara S, Imai T, Hamaguchi K, Okabe M, Aruga J, Nakajima K, et al. Mouse-Musashi-1, a neural RNA-binding protein highly enriched in the mammalian CNS stem cell. Dev. Biol. 1996; 176:230–242. [PubMed: 8660864]

Seki T, Arai Y. Distribution and possible roles of the highly polysialylated neural cell adhesion molecule (NCAM-H) in the developing and adult central nervous system. Neurosci. Res. 1993; 17:265–290. [PubMed: 8264989]

Seri B, Garcia-Verdugo JM, Collado-Morente L, McEwen BS, Alvarez-Buylla A. Cell types, lineage, and architecture of the germinal zone in the adult dentate gyrus. J. Comp. Neurol. 2004; 478:359–378. [PubMed: 15384070]

Shruster A, Melamed E, Offen D. Neurogenesis in the aged and neurodegenerative brain. Apoptosis. 2010; 15:1415–1421. [PubMed: 20339917]

Thal DR, Rub U, Orantes M, Braak H. Phases of A beta-deposition in the human brain and its relevance for the development of AD. Neurology. 2002; 58:1791–1800. [PubMed: 12084879]

von Bohlen Und Halbach O. Immunohistological markers for staging neurogenesis in adult hippocampus. Cell Tissue Res. 2007; 329:409–420. [PubMed: 17541643]

Winner B, Kohl Z, Gage FH. Neurodegenerative disease and adult neurogenesis. Eur. J. Neurosci. 2011; 33:1139–1151. [PubMed: 21395858]

Yu Y, He J, Zhang Y, Luo H, Zhu S, Yang Y, et al. Increased hippocampal neurogenesis in the progressive stage of Alzheimer's disease phenotype in an APP/PS1 double transgenic mouse model. Hippocampus. 2009; 19:1247–1253. [PubMed: 19309037]

Zhang C, McNeil E, Dressler L, Siman R. Long-lasting impairment in hippocampal neurogenesis associated with amyloid deposition in a knock-in mouse model of familial Alzheimer's disease. Exp. Neurol. 2007; 204:77–87. [PubMed: 17070803]

Ziabreva I, Ballard CG, Aarsland D, Larsen JP, McKeith IG, Perry RH, Perry EK. Lewy body disease: thalamic cholinergic activity related to dementia and parkinsonism. Neurobiol. Aging. 2006; 27:433–438. [PubMed: 15913843]

Europe PMC Funders Author Manuscripts

Europe PMC Funders Author Manuscripts

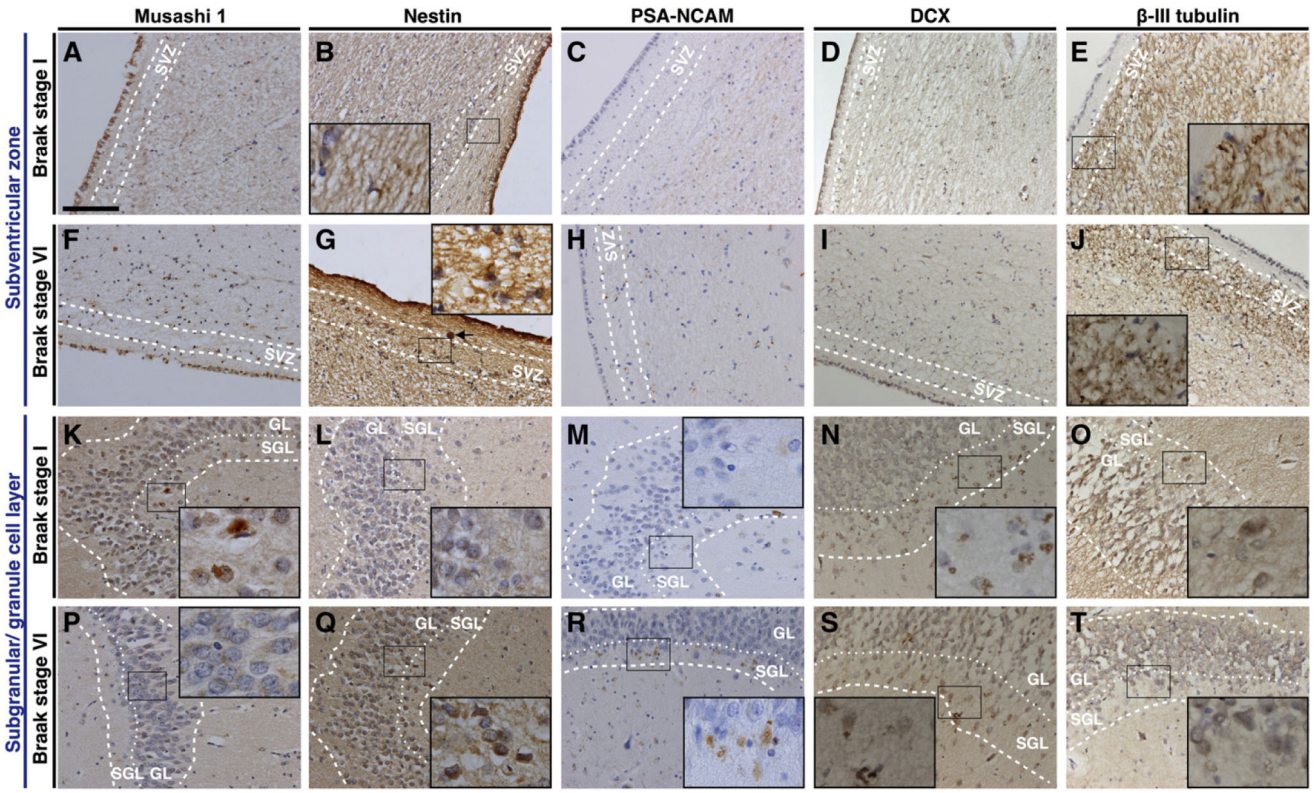

Fig. 1.

Musashi-1, Nestin and PSA-NCAM in Braak stages I and VI. Immmunoreactivity for each Musashi-1 (Msi-1), Nestin, and PSA-NCAM presented as positive staining in both neuronal somata and cellular processes. In the subventricular zone (SVZ) immunoreactivity for both Musashi-1 (Msi-1) and PSA-NCAM was similar in Braak stage I (A, Msi-1; C, PSA-NCAM) and Braak stage VI (D, Msi-1; F, PSA-NCAM) while nestin immunoreactivity was greater in E) Braak stage VI compared to B) Braak stage I. In both the sub-granular layer (SGL) and granule cell layer (GL) Msi-1 immunoreactivity was higher in G) Braak stage I compared to J) Braak stage VI. Conversely, nestin and PSA-NCAM immunoreactivity was lower in Braak stage I (H, nestin; I, PSA-NCAM) compared to Braak stage VI (K, nestin; L, PSA-NCAM). Sections were stained with polyclonal Msi-1 (A, D, G, J), polyclonal nestin (B, E, H, K) and monoclonal PSA-NCAM (C, F, I, L) antibodies the immunoreactive product was visualized by DAB/peroxide. Arrow in E indicates a corpus amylaceum that was not included into the measurement of immunoreactivity, likewise the areas measured did not include positive ependymal cells. Dashed lines indicate borders of SVZ, SGL, and GL as indicated and dotted lines mark the border between SGL and GL. Scale bar in A for A to T, 100 μm.

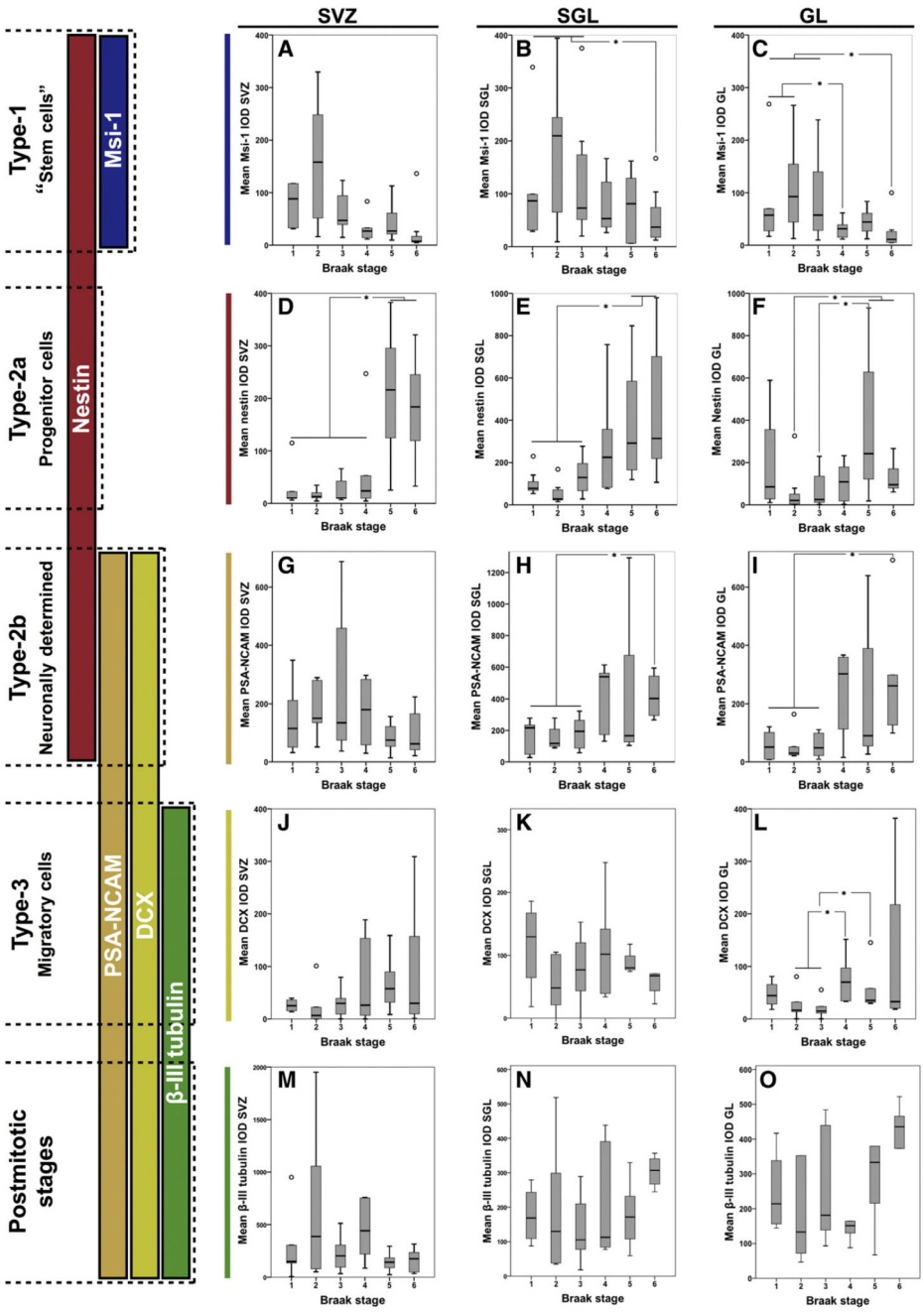

Fig. 2.

Mean Musahsi-1, nestin, PSA-NCAM, doublecortin, and β-III-tubulin immunoreactivity in Braak stages I to VI.Developmental stages in adult hippocampal neurogenesis are shown on the left side (see Kempermann, 2011). For further details regarding cell types 1–3 and postmitotic stages see main text. A) In the subventricular zone (SVZ) Musashi-1 (Msi-1) IOD did not differ significantly between Braak stages while in both B) sub-granular layer (SGL) and C) granular layer (GL) Msi-1 IOD decreased significantly with increasing Braak stages (SGL, rho=−0.413, P<0.01; GL, rho=−0.556, P<0.01). Nestin IOD significantly

increased with increasing Braak stages in D) SVZ (rho=0.666, P<0.01), E) SGL (rho=0.377, P<0.05), and F) GL (rho=0.646, P<0.01). No significant differences between Braak stages were seen for PSA-NCAM IOD in G) the SVZ. In the H) SGL (rho=0.489, P<0.01) and I) GL (rho=0.526, P<0.01) PSA-NCAM IOD significantly increased with increasing Braak stages. Mean doublecortin (DCX) IOD in the L) GL was significantly higher in Braak stage IV compared to II and III and in V compared to III, respectively, but no significant correlation was seen between both DCX (J–L) and β-III-tubulin (M–O) IODs and Braak stages. *, P<0.05; rings, outliers.

Europe PMC Funders Author Manuscripts

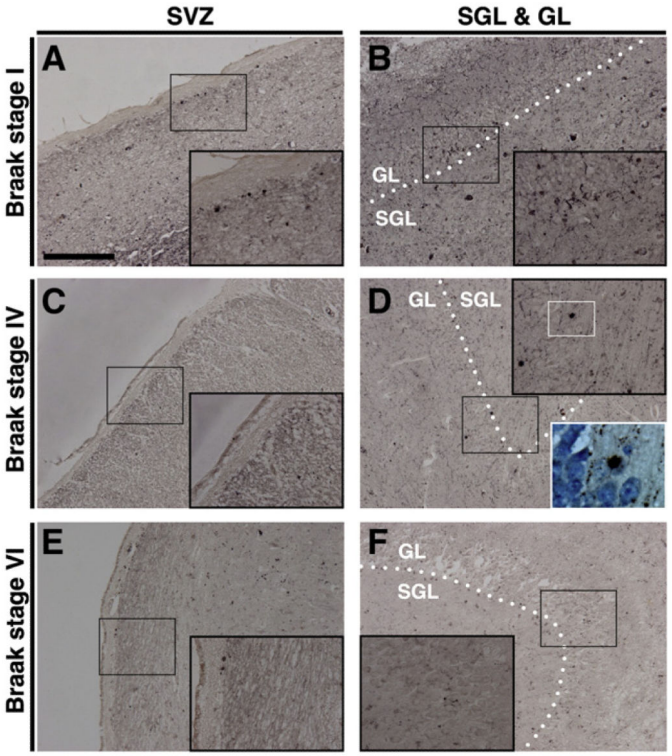

Fig. 3.

Choline acetyltransferase in Braak stages I, IV, and VI. Choline acetyltransferase (ChAT) immunoreactivity in the subventricular zone (SVZ) did not show differences between A) Braak stage I, C) Braak stage IV and E) Braak stage VI, while in both the subgranular layer (SGL) and the granule cell layer (GL) ChAT immunoreactivity decreased from B) Braak stage I to D) Braak stage IV and F) Braak stage VI. Lower right hand inset in D): Hematoxylin counterstain visualizes nuclei that are sometimes adjacent to strong globular cytoplasmic immunopositivity. Sections were incubated with polyclonal ChAT antibody and the immunoreactive product was visualized by nickel enhanced 3,3-diaminobenzidine; hematoxylin counterstain in the lower right inset in D; dotted line in B, D and F indicates border between SGL and GL; scale bar in A for A to F, 200 μm.

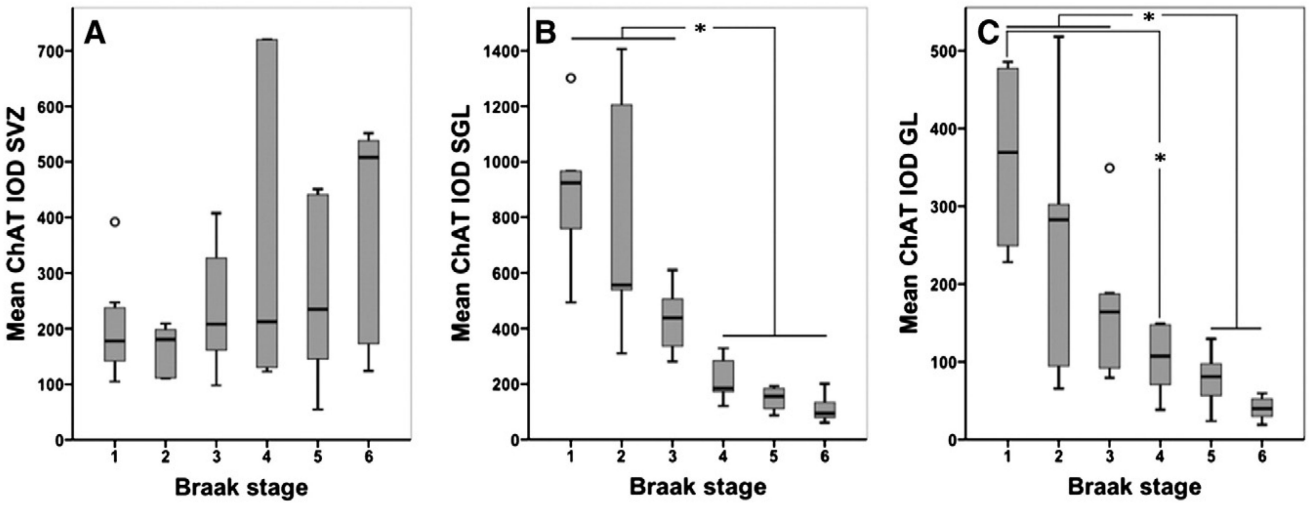

Fig. 4.

Mean choline acetyltransferase immunoreactivity in Braak stages I to VI.Box plots of mean choline acetyltransferase (ChAT) integrated optical density (IOD) show no significant differences between Braak stages in A) the subventricular zone (SVZ) but in both B) the sub-granular layer (SGL) and C) the granule cell layer (GL) ChAT IOD decreased significantly with increasing Braak stages (SGL, rho=−0.898; GL, rho=−0.79; $P<0.001$) and significant differences were seen in ChAT IOD between Braak stages I–III and IV–VI in the SGL (B) and between Braak stages I–III and V–VI as well as between I and IV in GL (C). *, $P<0.05$; rings, outliers.

Europe PMC Funders Author Manuscripts

Europe PMC Funders Author Manuscripts

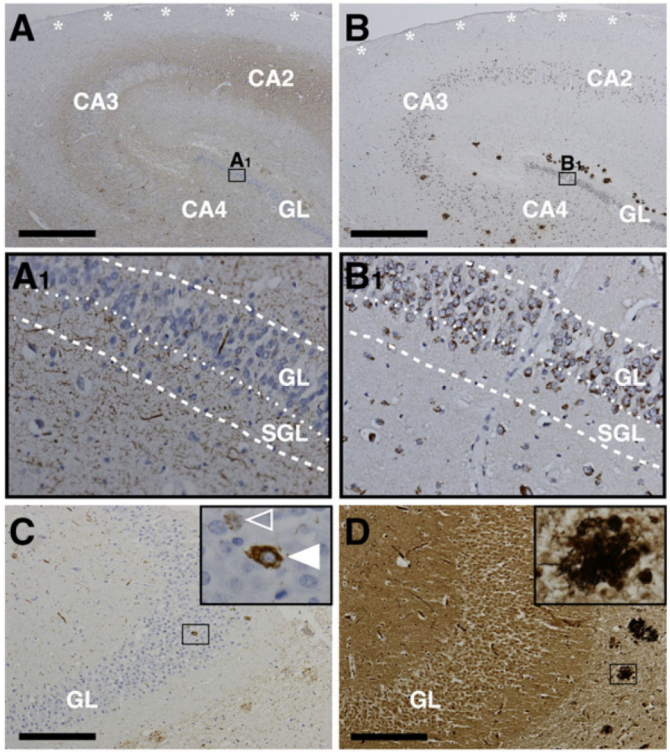

Fig. 5.

Alzheimer's disease neuropathology in neurogenic niche areas. The subventricular zone (SVZ) is devoid of Aβ-plaques, tau pathology, and neuritic plaques (asterisks in A and B). In both sub-granular layer (SGL) and granule cell layer (GL) hyperphosphorylated tau frequently presents as neuropil threads (thread-like immunopositivity in A1) while pretangles (open arrowhead in inset C) as well as neurofibrillary tangles (full arrowhead in inset C) are rarely seen and both Aβ-plaques (B1) and neuritic plaques (inset D) are completely absent. Of note, Aβ-antibody 4G8 reacts with the physiological transmembraneous amyloid precursor protein (APP) and therefore cellular immunopositivity in B1 does not reflect Aβ pathology but APP staining. Immuno-/histochemistry: A and C, AT8 (tau); B, 4G8 (Aβ); D, modified Bielschowsky silver stain. A–B and C–D are adjacent sections. Dashed lines indicate borders of SGL and GL as indicated and dotted lines mark border between SGL and GL. Scale bars: A and B, 1000 μm; C and D, 200 μm.

Europe PMC Funders Author Manuscripts

Table 1

Characteristics of the study group.

Braak stage	n	Age (mean±std)	Gender (male, female)	Clinical dementia
0–I	7	80.29±8.30	3, 4	0
II	7	81.28±10.24	2, 5	0
III	7	81.14±6.84	3, 4	0
IV	6	82.16±8.10	2, 4	6
V	7	79.57±5.31	3, 4	7
VI	7	81.85±7.56	2, 5	7
Total	41	81.05±7.73	15, 26	20

Table 2

Msi-1, netsin, PSA-NCAM, DCX, β-III-tubulin, and ChAT immunoreactivity.

	Total cohort (n=41)		Controls (n=21)		AD (n=20)		Control vs AD Mann–Whitney U
	Mean IOD	±SE	Mean IOD	±SE	Mean IOD	±SE	P value
Msi-1 SVZ	106.31	16.29	141.06	27.40	69.72	13.04	0.050
Msi-1 SGL	64.83	11.39	95.40	19.95	34.25	6.02	0.011
Msi-1 GL	91.00	22.03	146.85	39.90	35.15	8.42	0.001
nestin SVZ	250.26	46.78	98.87	16.79	409.23	80.84	<0.001
nestin SGL	159.04	35.28	98.89	35.90	213.17	56.95	0.019
nestin GL	91.20	17.86	24.45	6.31	154.61	27.81	<0.001
PSA-NCAM SVZ	154.72	25.88	199.50	44.80	109.94	22.25	0.122
PSA-NCAM SGL	306.20	48.48	170.03	23.89	427.23	79.61	0.005
PSA-NCAM GL	183.35	47.01	57.53	11.97	295.19	80.16	0.001
DCX SVZ	51.89	12.14	26.72	7.12	75.57	21.35	0.109
DCX SGL	97.56	15.38	78.56	14.31	115.45	26.40	0.387
DCX GL	58.39	13.02	29.20	6.35	85.87	22.92	0.004
β-III-tubulin SVZ	322.39	67.06	389.65	115.60	246.72	57.14	0.581
β-III-tubulin SGL	189.53	22.81	167.18	31.60	213.28	32.94	0.183
β-III-tubulin GL	315.69	48.11	266.66	52.60	367.78	81.83	0.418
ChAT SVZ	337.29	68.98	205.79	20.96	475.72	134.37	0.109
ChAT SGL	400.66	60.28	675.09	87.16	155.11	15.90	<0.001
ChAT GL	149.67	22.88	241.63	37.71	72.22	9.75	<0.001

Msi-1, musashi-1; DCX, doublecortin, ChAT, choline acetyltransferase; AD, Alzheimer's disease; SVZ, subventricular zone; SGL, sub-granular layer; GL, granule cell layer.